

# Diagnosing Pleural Effusion Caused by Silicosis in a Long-Term Quarry Worker: A Case Report

Xingxing Zhu<sup>1</sup>, Shengjie Wu<sup>2</sup>, Jiling Zeng<sup>3</sup>, Yahong Sun<sup>1</sup>, Jialu Chen<sup>4</sup>, Xiaohong Wu<sup>5</sup>

<sup>1</sup>Department of Pulmonary and Critical Care Medicine, Haining People's Hospital, Haining, People's Republic of China; <sup>2</sup>Department of Pharmacy, Sir Run Run Shaw Hospital, Zhejiang University School of Medicine, Hangzhou, People's Republic of China; <sup>3</sup>Department of Pathology, Sir Run Run Shaw Hospital, Zhejiang University School of Medicine, Hangzhou, People's Republic of China; <sup>4</sup>Department of Gynaecology, Haining Maternal and Child Health Hospital, Haining, People's Republic of China; <sup>5</sup>Department of Respiratory and Critical Care Medicine, Sir Run Run Shaw Hospital, Zhejiang University School of Medicine, Hangzhou, People's Republic of China

Correspondence: Xiaohong Wu, Department of Respiratory and Critical Care Medicine, Sir Run Run Shaw Hospital, Zhejiang University School of Medicine, No. 3 Qingchun East Road, Shangcheng District, Hangzhou, 310000, People's Republic of China, Tel +86 13588706901, Email 3192018@zju.edu.cn

**Background:** Patients affected by silicosis often exhibit clinical symptoms such as dyspnea, chronic cough, sputum production, hemoptysis, and chest pain. Common complications of silicosis include pulmonary tuberculosis, right-sided heart failure, emphysema, and lung cancer. Some of these complications can cause pleural effusion, however, reports that clearly attribute pleural effusion directly to silicosis are uncommon. We report a case of pleural effusion directly caused by silicosis, confirmed by thoracoscopic pleural biopsy and polarized microscopy.

**Case Description:** We report a case of a 78-year-old man with a history of working in a quarry for over 10 years. He was admitted to our hospital twice due to chest tightness and dyspnea. Both chest computed tomography (CT) scans indicated multiple nodular changes in the lungs, with predominantly right-sided pleural effusion. The results of pleural fluid tests were consistent with exudative effusion. Pleural biopsy specimens obtained by thoracoscopy showed silica particles under polarized light microscopy. Additional tests ruled out heart failure, tumors, and other causes of pleural effusion, based on which a final diagnosis of pleural effusion due to silicosis was made.

**Conclusion:** This case provides histological proof that silicosis can directly involve the pleura and cause exudative effusion. Furthermore, it highlights the diagnostic value of thoracoscopic pleural biopsy with polarized microscopy in silica-exposed patients with unexplained pleural effusion.

**Keywords:** silicosis, silica, pleural effusion, thoracoscopy, pleural biopsy

## Introduction

Silicosis is a type of pneumoconiosis caused by prolonged occupational exposure to reactive crystalline silica that leads to interstitial lung disease.<sup>1</sup> Various occupations are closely related to the risk of silicosis, including quarrying, mining, stone cutting, sandblasting, grinding, construction, denim sandblasting, and artificial stone countertop manufacturing.<sup>2,3</sup> The Global Burden of Disease 2016 estimated that silicosis is responsible for around 10,400 deaths annually.<sup>2</sup> In 2017, silicosis was highly prevalent, representing 39% (23,695 cases) of all new pneumoconiosis cases globally.<sup>4</sup>

Macrophages play a central role in the development of silicosis. When macrophages ingest dust particles to the point of overload, they can no longer absorb silica particles. This leads to macrophage swelling, which promotes chronic inflammation and gradually leads to silicosis.<sup>5</sup> Early lesions present as cellular nodules composed of fibroblasts and tissue cells that contain a large number of silica particles.<sup>6</sup> Silica particles are deposited in the lungs mainly after inhalation through the airways, but they may also reach the pleura via the lymphatic system and through the bloodstream.<sup>7</sup> Silica particles can induce oxidative stress in pleural mesothelial cells, resulting in cellular injury and the release of inflammatory mediators.<sup>8</sup> Common clinical symptoms of silicosis include dyspnea, chronic cough, sputum production, hemoptysis, and chest pain, and the common complications are pulmonary tuberculosis, right heart failure, pneumothorax, and lung cancer.<sup>3,9</sup> Some of these complications can cause pleural effusion, such as pulmonary

tuberculosis, right heart failure and lung cancer. However, pleural effusion is a uncommon complication caused directly by silicosis, with only a few detailed reports published so far.<sup>10–13</sup> Here, we report a case of pleural effusion caused by silicosis. We believe that the findings are important given the rarity of such case reports, as they could guide timely diagnosis and treatment in the future.

## Case Presentation

The patient is a 78-year-old Han Chinese (Asian) man who presented with exertional chest tightness and dyspnea. He had been experiencing this for over a month. On May 16, 2023, he visited our outpatient department, where a chest CT revealed diffuse patchy and nodular increased density shadows, with pleural effusion predominantly observed on the right side (Figure 1A–D). An electrocardiogram showed atrial fibrillation with a normal ventricular rate (average, 78 beats/min). He was subsequently admitted for further evaluation and treatment. The patient had worked in a quarry for approximately 10 years and presented with chest tightness and dyspnea approximately 28 years after cessation of silica exposure. He also had a 30-year history of smoking (20 cigarettes per day) and had quit 1 year prior to presentation. Upon admission, his vital signs were as follows: blood pressure, 157/79 mm Hg; ear temperature, 37.0°C; and respiratory rate, 19 breaths/min. Auscultation revealed decreased breath sounds with some fine rales, and there was no facial or lower limb edema. The results of laboratory tests upon admission were as follows: white blood cell count:  $3.5 \times 10^9/L$ , high-sensitivity C-reactive protein: 10.7 mg/L, erythrocyte sedimentation rate: 47 mm/h, procalcitonin: 0.06 ng/mL, N-terminal pro-B-type natriuretic peptide (NT-proBNP): 1249 pg/mL, total protein: 67.1 g/L, albumin: 33.5 g/L, lactate dehydrogenase: 214 IU/L, Carbohydrate Antigen 125 (CA 125): 147.6 U/mL (Table 1). The results of liver and kidney function tests, electrolyte analysis, and routine urinalysis were normal. The results of tests for hepatitis B, hepatitis C, Human Immunodeficiency Virus (HIV), and syphilis were negative. Echocardiography revealed enlargement of both atria, left ventricular hypertrophy, moderate tricuspid regurgitation with severe pulmonary hypertension, and mild to moderate pericardial effusion (Figure 2A). Bilateral pleural effusion ultrasonography showed approximately 1.4 cm deep fluid collection in the left pleural cavity and approximately 7.02 cm deep fluid collection in the right pleural cavity (Figure 3A and B).

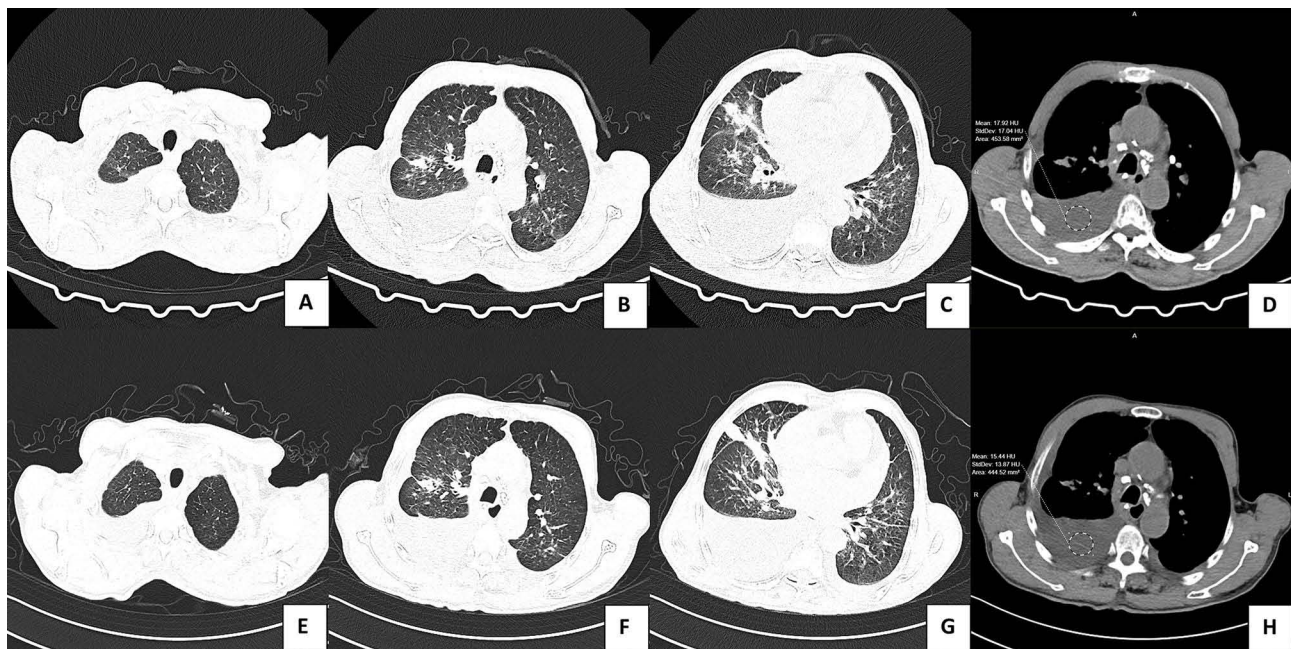


**Figure 1** Chest CT taken at both hospital admissions. (A–D) Chest CT taken on May 16, 2023: Both lungs show diffuse patchy, nodular, and linear increased opacities; bilateral pleural effusions (right-predominant) with adjacent atelectasis; calcified mediastinal lymph nodes. In panel D, the right-sided pleural effusion shows a mean CT attenuation of 17.92 HU. (E–H) Chest CT taken on September 10, 2023: Similar findings are present: diffuse patchy, nodular, and linear increased opacities in both lungs; bilateral pleural effusions (right-predominant) with adjacent atelectasis; calcified mediastinal lymph nodes. In panel H, the right-sided pleural effusion shows a mean CT attenuation of 15.44 HU.

**Table 1** Blood Test Results at Both Hospital Admissions

Blood Parameters (Normal Values Shown in Parentheses)	First Admission (May 16, 2023)	Second Admission (September 8, 2023)
White Blood Cell Count ( $3.5\text{--}9.5 \times 10^9/\text{L}$ )	3.5	3.8
Hemoglobin Concentration (130–175 g/L)	128	121
Platelet Count ( $125\text{--}350 \times 10^9/\text{L}$ )	156	157
High-Sensitivity C-Reactive Protein (<6.0 mg/L)	10.7	14.5
Erythrocyte Sedimentation Rate (1–15 mm/h)	47	52
Procalcitonin (<0.05 ng/mL)	0.06	0.04
NT-proBNP (<1800 pg/mL)	1249	1765
High-Sensitivity Troponin (<54 ng/L)	16	54
Total Protein (65.0–85.0g/L)	67.1	67.8
Albumin (40.0–55.0g/L)	33.5	34.9
Lactate Dehydrogenase (120–250 IU/L)	214	232
Prothrombin Time (11.5–14.5 s)	14.8	15
International Normalized Ratio (0.90–1.10)	1.18	1.2
D-Dimer (<0.50 $\mu\text{g}/\text{mL}$ )	1.35	1.94
Fibrinogen (2.00–4.00 g/L)	4.06	4.28
Cancer Antigen 125 (<35.00 U/mL)	147.6	97.31

On May 22, 2023, ultrasound imaging revealed right-sided pleural effusion. The pleural fluid was yellow and slightly turbid, with the analysis indicating exudative effusion: white blood cells:  $2420/\mu\text{L}$ , lymphocyte percentage: 92.0%, lymphocyte test: positive (+), adenosine deaminase: 10.0 IU/L, pleural fluid lactate dehydrogenase: 149 IU/L, total protein in pleural fluid: 44 g/L (Table 2). Cultures of the pleural fluid did not reveal bacterial or fungal growth. Pleural fluid cytological analysis showed a few atypical cells that exhibited the features of reactive mesothelial cells.

On May 25, 2023, a Positron Emission Tomography-Computed Tomography(PET-CT) scan showed diffuse patchy and nodular lesions in both lungs, some show increased FDG uptake, favoring an inflammatory etiology. In addition, multiple calcified lymph nodes are present in the mediastinum and bilateral hila (Figure 4). Chest tube drainage was performed, and the patient's symptoms improved. He was discharged after tube removal and started on long-term oral anticoagulant therapy with rivaroxaban for atrial fibrillation.

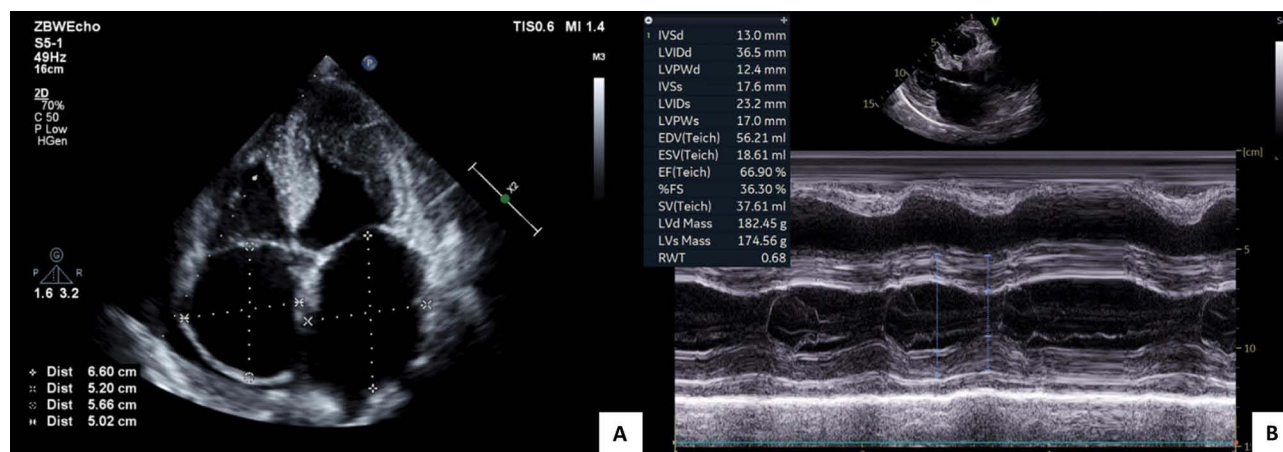


**Figure 2** Echocardiograms taken at both hospital admissions. (A) Echocardiogram taken on May 21, 2023: Ejection Fraction (EF): 72.8%, Ascending Aorta(AAO): 32.5 mm, Aorta(AO): 25.1 mm, Left Atrium(LA): 66.052.044.7 mm, Right Atrium(RA): 56.650.2 mm, Pulmonary Artery(PA): 18.7 mm, Right Ventricular Systolic Pressure(RVSP): 74 mmHg. The image shows enlarged atria, atrial fibrillation, left ventricular hypertrophy, moderate tricuspid regurgitation with severe pulmonary hypertension, degenerative changes in the aortic valve with mild regurgitation, degenerative changes in the mitral valve with mild regurgitation, and mild to moderate pericardial effusion. (B) Echocardiogram taken on September 9, 2023: EF: 66.9%, AAO: 33.0 mm, AO: 27.4 mm, LA: 62.746.945.3 mm, RA: 63.746.1 mm, PA: 25.7 mm, RVSP: 62 mm Hg. The image shows enlarged atria, atrial fibrillation, left ventricular hypertrophy, moderate tricuspid regurgitation with moderate pulmonary hypertension, degenerative changes in the aortic valve with mild regurgitation, degenerative changes in the mitral valve with mild regurgitation, and mild to moderate pericardial effusion.

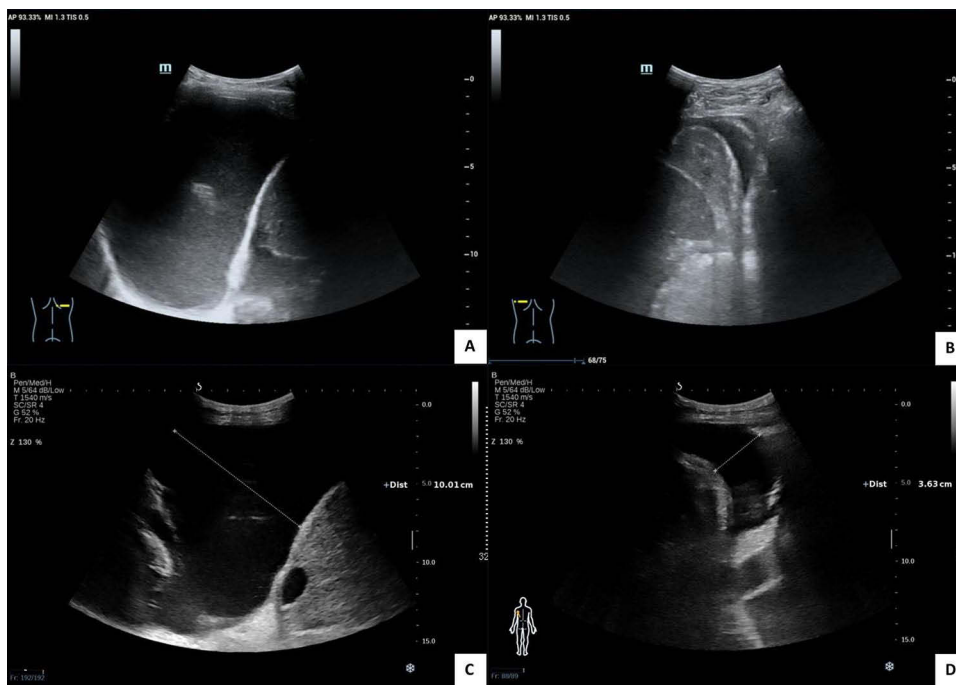


**Figure 3** Ultrasound images taken at both hospital admissions. **(A and B)** Ultrasound images taken on May 21, 2023 showing bilateral pleural effusion. The images show a fluid-filled dark area approximately 1.4 cm deep in the left thoracic cavity and a fluid-filled dark area approximately 7.02 cm deep in the right thoracic cavity. **(C and D)** Ultrasound images taken on September 11, 2023, showing bilateral pleural effusion. The images show a fluid-filled dark area approximately 3.63 cm deep in the left thoracic cavity and a fluid-filled dark area approximately 10.01 cm deep in the right thoracic cavity.

The patient was readmitted on September 8, 2023, due to worsening of the chest tightness and dyspnea over the past week. On admission, his vital signs were as follows: blood pressure, 157/102 mm Hg; ear temperature, 36.4°C; and respiratory rate, 19 breaths/min. Physical examination revealed decreased breath sounds with some fine rales, and there was no lower limb edema. Laboratory tests upon readmission indicated that the C-reactive protein(CRP) concentration and erythrocyte sedimentation rate were slightly elevated compared to the previous results. However, the white blood cell count and procalcitonin levels

**Table 2** Pleural Effusion Test Results at Both Hospital Admissions

Pleural Fluid	First Admission (May 16, 2023)	Second Admission (September 8, 2023)
Red Blood Cells (/μL)	1000	100
White Blood Cells (/μL)	2420	1357
Neutrophils (%)	5	1
Lymphocytes (%)	92	89
Eosinophils (%)	0	0
Mesothelial Cells (%)	0	1
Macrophages (%)	3	10
Leflunomide Test	Positive	Weakly Positive
Total Protein (g/L)	44	38
Albumin (g/L)	24	21
Lactate Dehydrogenase (IU/L)	149	99
Adenosine Deaminase (IU/L)	10	8
Glucose (mmol/L)	6.41	6.14
Carcinoembryonic Antigen (ng/mL)	2.05	1.10

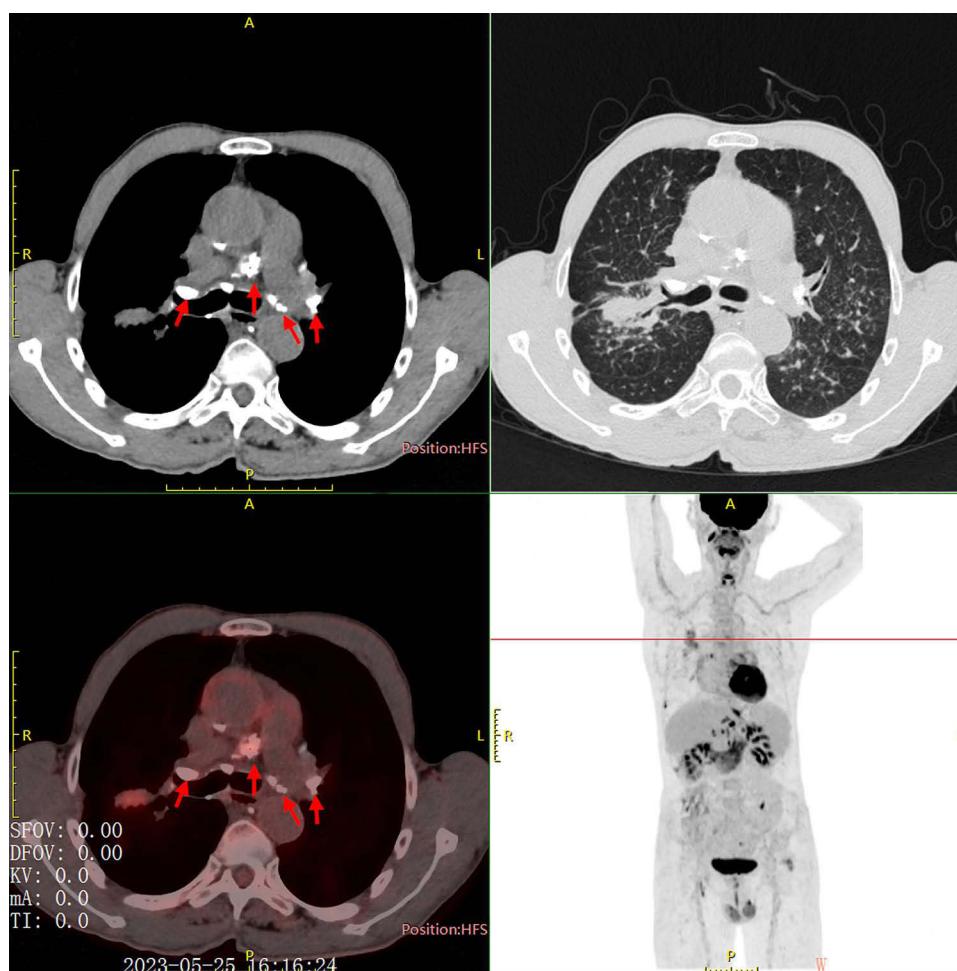


**Figure 4** PET-CT image taken at the first hospital admission. PET-CT whole-body image taken on May 25, 2023 showing diffuse patchy and nodular lesions in both lungs, some show increased FDG uptake, favoring an inflammatory etiology. In addition, multiple calcified lymph nodes in the mediastinum and bilateral hila. The structures indicated by red arrows correspond to mediastinal calcified lymph nodes.

were normal, with no evidence of bacterial infection. NT-proBNP showed a slight increase but remained within the normal range. The CA 125 level had decreased compared to previous results (Table 1). Electrocardiography revealed atrial fibrillation with a normal ventricular rate (average, 80 beats/min). Chest CT indicated that the lung nodules and pleural effusion were similar to the previous findings (Figure 1E–H). Echocardiography showed a reduction in pulmonary artery pressure compared to the last examination, and the other indicators were largely unchanged (Figure 2B). Ultrasound imaging of bilateral pleural effusion demonstrated persistent bilateral effusion that was predominant on the right side (Figure 3C and D).

Right-sided pleural puncture and drainage were performed under ultrasound guidance, and fluid analysis confirmed the presence of exudative fluid (Table 2). Pleural fluid culture showed that there was no bacterial or fungal growth. Cytological examination of the pleural fluid indicated the presence of a small number of atypical cells. Further, right-sided thoracoscopic pleural biopsy revealed slight black pigment deposition on the parietal pleura (Figure 5). The parietal pleura was biopsied to extract seven samples, all of which exhibited bright white silica crystals of varying sizes under a polarized microscope (Figure 6). Following closed chest drainage and diuretic therapy, the patient experienced improvement in chest tightness and dyspnea and was subsequently discharged.

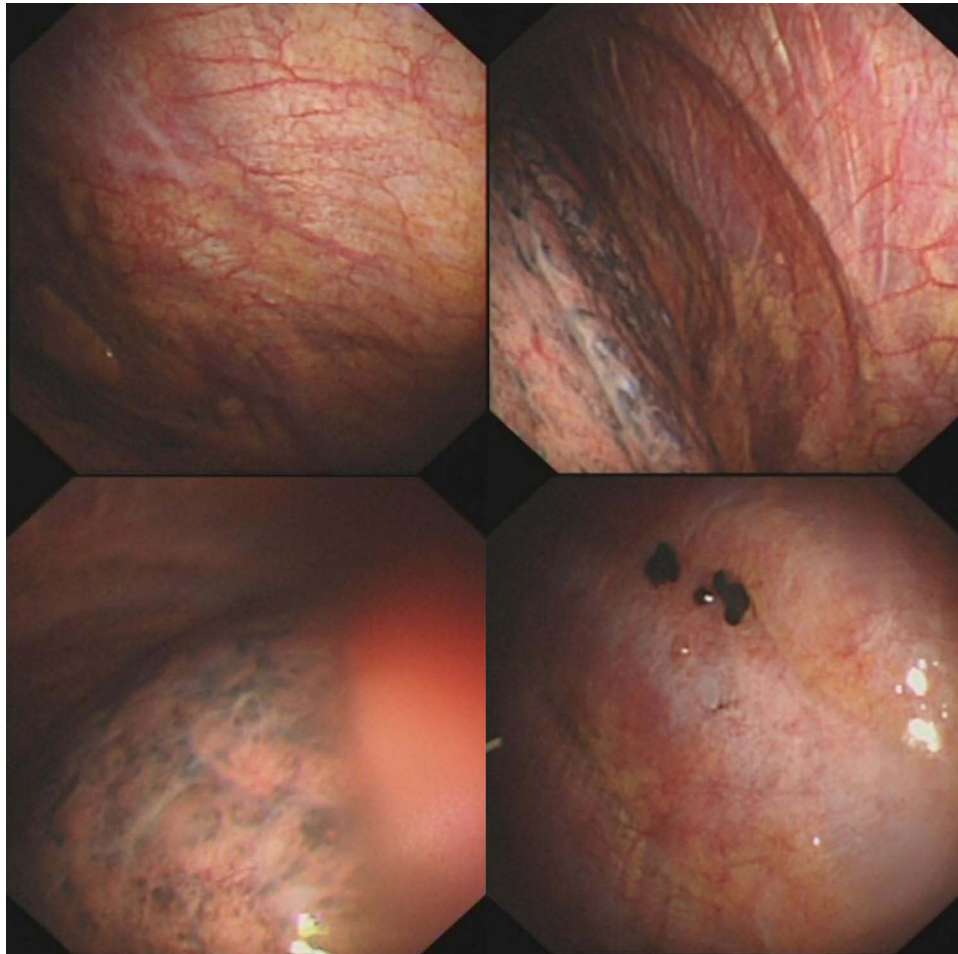


**Figure 5** Thoroscopic image taken at the second hospital admission. Right thoracoscopy with pleural biopsy performed on September 12, 2023, showing black pigment deposition in the parietal pleura.

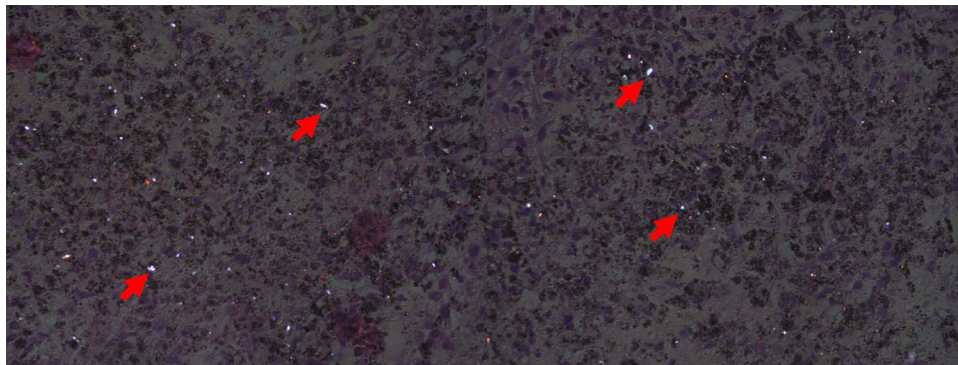


**Figure 6** Pathology of pleural biopsy under thoracoscopy. Right thoracoscopy with pleural biopsy performed on September 20, 2023 showing bright white silicon dioxide crystals of varying sizes under a polarized microscope. Red arrows indicate representative silica crystals.

## Discussion

The present report describes a case of silicosis that led to pleural effusion in a quarry worker with long-term occupational exposure to silica dust. The symptoms and presentations, imaging features, and treatment outcomes described here could be useful for clinicians considering the rarity of such case reports.

The high resolution computed tomography (HRCT) imaging characteristics of silicosis primarily include nodular changes in the lung parenchyma, progressive large-area fibrosis, lung bullae, emphysema, and changes in lymph nodes and pleura.<sup>14</sup> Different types of silicosis also have distinct features on HRCT images. Acute silicosis is mainly characterized by extensive ground-glass opacities that are often accompanied by large areas of consolidation and varying degrees of centrilobular nodules and reticular patterns.<sup>15</sup> Simple silicosis primarily presents with small nodules ranging from 2 to 5 mm in diameter in the centrilobular regions, but may also show nodules distributed along lymphatic vessels or peripherally, with possible mediastinal lymph node enlargement or eggshell-like calcification.<sup>16–18</sup> Complicated silicosis mainly presents as progressive massive fibrosis, where the small nodules in simple silicosis coalesce into larger masses with diameters of 10 mm or more and may show pleural thickening or pleural plaques.<sup>16,18</sup> Accelerated silicosis mainly shows changes in ground-glass opacities superimposed on simple silicosis and may also exhibit corresponding emphysema, with some cases showing progressive massive fibrosis.<sup>16,19</sup> Pleural effusion is a uncommon manifestation of silicosis that is primarily seen in cases of simple silicosis.<sup>18</sup> In our case, the patient's chest CT showed multiple central nodules in both lungs, enlarged and calcified mediastinal lymph nodes, and right-sided pleural effusion, consistent with the imaging features of simple silicosis.

As mentioned earlier, reports on pleural effusion caused by silicosis remain relatively scarce, diagnoses rely on imaging and lack direct histological confirmation.<sup>18</sup> Our case is notable for the use of thoracoscopic pleural biopsy to confirm pleural effusion due to silicosis, as this diagnostic technique is less commonly reported. Additionally, current studies on the nature of pleural fluid in silicosis are limited, although all of them suggest that the effusion is exudative.<sup>10,12,13</sup> Consistent with these cases, the pleural effusion was confirmed to be exudative in the present case. Moreover, thoracoscopic biopsy confirmed that the exudative pleural effusion was caused by pleural involvement of silicosis. Despite the presence of pulmonary hypertension and atrial fibrillation, the patient did not have lower limb edema. Moreover, his NT-proBNP levels were normal at both hospital admissions; echocardiography showed normal ejection fraction(EF); and the effusion was transudative. Based on these findings, heart failure was ruled out as the cause of the pleural effusion. PET-CT did not reveal any lung tumors, and no malignant cells were found in the pleural fluid. Based on these observations, tumor-related effusion was excluded. Furthermore, silica particles were identified in the biopsy tissue, further confirming that the pleural effusion was due to silicosis.

The interval from silica exposure to the development of silicosis can range from several years to several decades and depends mainly on the duration and intensity of exposure. Chronic silicosis is the most common form and typically has a latency of 15–20 years or longer, whereas accelerated silicosis has a latency of approximately 5–10 years and acute silicosis develops within a few months to 2 years.<sup>20</sup> Because genetic and epigenetic makeup differs between individuals, people working in the same environment and exposed to identical levels of silica dust can have different susceptibilities to silicosis.<sup>21</sup> In this case, the patient had approximately 10 years of silica exposure and presented with chest tightness and dyspnea about 28 years after exposure cessation. Because routine occupational health follow-up and imaging screening were lacking, silicosis likely developed before the 28-year mark but went unrecognized due to absent or mild symptoms. Silicosis can continue to progress after exposure ends, which explains the onset of symptoms many years later and the eventual diagnosis. Overall, the timeline in this patient aligns with the natural history of chronic silicosis.

The mechanisms behind pleural effusion caused by silicosis involve multiple factors. For example, Zhu et al created rat models of pleural and pericardial effusion by administration of polyacrylate/silica nanoparticles, with a dose-dependent effect, and proposed three possible mechanisms: inflammation and reactive oxygen species production, lymphatic obstruction, and direct damage to microlymphatics that affects lymphatic formation and fluid reabsorption.<sup>22</sup> Our case also presented with both pleural and pericardial effusions, similar to Zhu et al's animal studies, but the specific mechanisms in human silicosis-related effusions remain unclear and require further investigation.

One of the main limitations of this report is that although PET-CT and pleural fluid cytology helped rule out malignancy to some extent, we did not perform a biopsy of the lung nodules to further exclude the possibility of malignancy. Nonetheless, the pleural biopsy and other extensive analyses performed in this case allowed for detailed differential diagnosis and provide a fairly definitive diagnosis. An additional limitation is that we did not analyze or quantify the concentration of silica crystals in the pleural effusion. We also did not compare these findings with

effusions of other etiologies, such as malignant pleural effusion, bacterial pleural effusion, and benign asbestos-related pleural effusion. In the absence of such comparative data and standardized analytic methods, we cannot determine the specificity or diagnostic value of pleural fluid silica burden for differentiating causes of pleural disease.

## Conclusion

To conclude, we describe a uncommon case of pleural effusion caused directly by silicosis in which pleural biopsy was used to confirm that the effusion was caused by silicosis and other analyses were used to rule out other potential causes of the pleural effusion. We believe that the findings presented here would be valuable to clinicians who encounter such cases in the future.

## Data Sharing Statement

This article provides a detailed account of the original data for this case report, which can be shared without requiring institutional approval. For additional information, please contact the corresponding authors.

## Ethics Approval and Informed Consent

This study was reviewed and approved by the Ethics Committee of Sir Run Run Shaw Hospital, Zhejiang University School of Medicine, China. Written informed consent has been provided by the patient to have the case details and any accompanying images published. Institutional approval was not required to publish the case details.

## Acknowledgments

We sincerely appreciate the patient's active cooperation throughout the entire treatment process and their willingness to actively participate in our study.

## Funding

This research was supported by Zhejiang Provincial Natural Science Foundation of China under Grant No.LQ22H010001 and National Key Research and Development Program Grant No. 2022YFC3601001.

## Disclosure

The authors report no conflicts of interest in this work.

## References

1. Vanka KS, Shukla S, Gomez HM, et al. Understanding the pathogenesis of occupational coal and silica dust-associated lung disease. *Eur Respir Rev.* 2022;31(165):210250. doi:10.1183/16000617.0250-2021
2. Hoy RF, Chambers DC. Silica-related diseases in the modern world. *Allergy.* 2020;75(11):2805–2817. doi:10.1111/all.14202
3. Churg A, Muller NL. Update on Silicosis. *Surg Pathol Clin.* 2024;17(2):193–202. doi:10.1016/j.path.2023.11.005
4. Shi P, Xing X, Xi S, et al. Trends in global, regional and national incidence of pneumoconiosis caused by different aetiologies: an analysis from the global burden of disease study 2017. *Occup Environ Med.* 2020;77(6):407–414. doi:10.1136/oemed-2019-106321
5. Zhao JH, Li S, Du SL, Zhang ZQ. The role of mitochondrial dysfunction in macrophages on SiO<sub>2</sub>-induced pulmonary fibrosis: a review. *J Appl Toxicol.* 2024;44(1):86–95. doi:10.1002/jat.4517
6. Nakano-Narusawa Y, Yokohira M, Yamakawa K, Saoo K, Imaida K, Matsuda Y. Single intratracheal quartz instillation induced chronic inflammation and tumorigenesis in rat lungs. *Sci Rep.* 2020;10(1):6647. doi:10.1038/s41598-020-63667-4
7. Ferrer J, Orriols R, Tura JM, Lirola J, Xaus C, Vidal X. Energy-dispersive X-ray analysis and scanning electron microscopy of pleura. Study of reference, exposed non-pneumoconiotic, and silicotic populations. *Am J Respir Crit Care Med.* 1994;149(4 Pt 1):888–892. doi:10.1164/ajrccm.149.4.8143051
8. Berg JM, Romoser AA, Figueroa DE, Spencer West C, Sayes CM. Comparative cytological responses of lung epithelial and pleural mesothelial cells following in vitro exposure to nanoscale SiO<sub>2</sub>. *Toxicol In Vitro.* 2013;27(1):24–33. doi:10.1016/j.tiv.2012.09.002
9. Kabamba Ngombe L, Nlandu Ngatu R, Nyembo Mukena C, et al. Silicosis in underground miners in Lubumbashi, Democratic Republic of the Congo: 27 cases. *Med Sante Trop.* 2018;28(4):395–398. doi:10.1684/mst.2018.0812
10. al-Kassimi FA. Pleural effusion in silicosis of the lung. *Br J Ind Med.* 1992;49(6):448–450. doi:10.1136/oem.49.6.448
11. Zeren EH, Colby TV, Roggli VL. Silica-induced pleural disease: an unusual case mimicking malignant mesothelioma. *Chest.* 1997;112(5):1436–1438. doi:10.1378/chest.112.5.1436

12. Salih M, Aljarod T, Ayan M, Jeffrey M, Shah BH. Pulmonary silicosis presents with pleural effusion. *Case Rep Med.* 2015;2015:543070. doi:10.1155/2015/543070
13. Okamoto S, Kobayashi I, Moriyama H, et al. Silicosis-related pleural effusion diagnosed using elemental analysis of the pleural fluid cell block: a case report. *Respir Med Case Rep.* 2022;37:101665. doi:10.1016/j.rmcr.2022.101665
14. Leung CC, Yu IT, Chen W. Silicosis. *Lancet.* 2012;379(9830):2008–2018. doi:10.1016/S0140-6736(12)60235-9
15. Batra K, Aziz MU, Adams TN, Godwin JD. Imaging Of Occupational Lung Diseases. *Semin Roentgenol.* 2019;54(1):44–58. doi:10.1053/j.ro.2018.12.005
16. Jones CM, Pasricha SS, Heinze SB, MacDonald S. Silicosis in artificial stone workers: spectrum of radiological high-resolution CT chest findings. *J Med Imaging Radiat Oncol.* 2020;64(2):241–249. doi:10.1111/1754-9485.13015
17. Cox CW, Rose CS, Lynch DA. State of the art: imaging of occupational lung disease. *Radiology.* 2014;270(3):681–696. doi:10.1148/radiol.13121415
18. Arakawa H, Honma K, Saito Y, et al. Pleural disease in silicosis: pleural thickening, effusion, and invagination. *Radiology.* 2005;236(2):685–693. doi:10.1148/radiol.2362041363
19. Grubstein A, Shtraichman O, Fireman E, Bachar GN, Noach-Ophir N, Kramer MR. Radiological Evaluation of Artificial Stone Silicosis Outbreak: emphasizing Findings in Lung Transplant Recipients. *J Comput Assist Tomogr.* 2016;40(6):923–927. doi:10.1097/RCT.0000000000000454
20. Handra CM, Gurzu IL, Chirila M, Ghita I. Silicosis: new challenges from an old inflammatory and fibrotic disease. *Front Biosci.* 2023;28(5):96. doi:10.31083/j.fbl2805096
21. Zhou Y, Zhang Y, Zhao R, et al. Integrating RNA-seq with GWAS reveals a novel SNP in immune-related HLA-DQB1 gene associated with occupational pulmonary fibrosis risk: a multi-stage study. *Frontiers in Immunology.* 2021;12:796932. doi:10.3389/fimmu.2021.796932
22. Zhu X, Cao W, Chang B, et al. Polyacrylate/nanosilica causes pleural and pericardial effusion, and pulmonary fibrosis and granuloma in rats similar to those observed in exposed workers. *Int J Nanomedicine.* 2016;11:1593–1605. doi:10.2147/IJN.S102020

### International Medical Case Reports Journal

### Publish your work in this journal

The International Medical Case Reports Journal is an international, peer-reviewed open-access journal publishing original case reports from all medical specialties. Previously unpublished medical posters are also accepted relating to any area of clinical or preclinical science. Submissions should not normally exceed 2,000 words or 4 published pages including figures, diagrams and references. The manuscript management system is completely online and includes a very quick and fair peer-review system, which is all easy to use. Visit <http://www.dovepress.com/testimonials.php> to read real quotes from published authors.

Submit your manuscript here: <https://www.dovepress.com/international-medical-case-reports-journal-journal>

**Dovepress**  
Taylor & Francis Group